Journal of Sound and Vibration (1998) **210**(5), 627–642

DYNAMICS OF A TIRE–WHEEL–SUSPENSION ASSEMBLY

C. R. Dohrmann

Mail Stop 0439, *Sandia National Laboratories*, *Albuquerque*, *NM* 87185-0439, *U.S.A.*

(*Received* 22 *January* 1997, *and in final form* 22 *September* 1997)

A method is presented for the dynamic analysis of a tire–wheel–suspension assembly. The suspension, modelled by linear spring and dashpot elements, is connected to the center of a rigid wheel rotating at a constant angular rate. The tire is modelled as an inextensible circular ring on a foundation connected to the wheel. A distinguishing feature of the method is that tire deformations are expressed as functions of a fixed-frame rather than a rotating-frame co-ordinate. With such an approach, the equations of motion are expressed as a linear, time-invariant system. This is in stark contrast to previously published results in which a parametrically excited system with periodic coefficients is obtained. Advantages of the method include: (1) stability can be determined from an eigenvalue analysis rather than from Floquet analysis which requires numerical time integration, and (2) modal characteristics of the system in rolling contact can be readily determined. Results are presented which show the effects of rotation and damping on the static response of a tire in rolling contact with a flat, frictionless surface. The effects of rotation on the frequencies and damping ratios of the system are also presented.

1. INTRODUCTION

Interactions between a vehicle and its tires can influence ride quality significantly. That being the case, a fundamental understanding of the motion of coupled vehicle–tire systems is key to accurately predicting ride response. The purpose of this paper is to add to this understanding by studying the dynamics of a tire–wheel–suspension assembly.

Tire–wheel systems that are not coupled to other structures have been studied extensively. Approaches to the dynamic analysis of tires include, among others, ring on elastic foundation models [1–5], thin shell models analyzed using dynamic Green's function approaches [6–7], and finite element models [8–12]. A study of the effects of stiffness non-uniformities on the dynamics of a tire in ground contact is provided in reference [13]. Coupled analyses have typically employed simplified idealizations of the tire such as lumped parameter [14] and ring [15] models.

A fundamental issue in the study of tire–vehicle systems is the form of the governing equations of motion. Admittedly, general purpose finite element codes can be used to formulate and solve the non-linear equations of motion for such systems, but the resources required can be prohibitive for purposes of ride simulation. Assuming linear models of the vehicle and tire, the question arises as to the form of the equations for the coupled system. Previous studies of a tire–wheel–suspension unit [15] indicated that the equations of motion assume the form of a parametrically excited system with periodic coefficients. In this study, the equations of motion are expressed as a linear, time-invariant system with constant coefficients.

0022–460X/98/100627 + 16 $25.00/0/sv971332

For purposes of simplicity, the tire is modelled as an inextensible circular ring on a foundation characterized by distributed spring and dashpot elements in the radial and tangential directions. This foundation can be viewed as a viscoelastic annulus which restrains relative motion between the wheel and the outer part of the tire. A rigid wheel rotating at a constant angular rate connects the tire to a suspension which is modelled by discrete linear springs and dashpots. Deformations of the system are restricted to motion within a plane.

A distinguishing feature of the method presented is that tire deformations are expressed as functions of a fixed-frame angular co-ordinate. Related kinematic descriptions have been adopted by others [16, 17] for rolling contact problems. An important consequence of using the fixed-frame approach is that the equations of motion can be expressed as a linear, time-invariant system.

In the following section, the equations of motion for the system are derived. Using a Fourier series approach, these equations are transformed to a set of simpler equations for each harmonic. Formulas for the undamped natural frequencies of the system not in ground contact, along with a method for stability analysis, are presented and compared with other approaches. In the third section, a method is presented for determining the static response of a tire in contact with a flat frictionless surface. The effects of damping and rotation rate on the contact solution are shown for an example problem. In the fourth section, a method is developed for determining the modal characteristics of a system in ground contact. The effects of the rotation rate on the natural frequencies and damping ratios of the system are shown.

2. EQUATIONS OF MOTION

The model used for the tire–wheel–suspension assembly is shown in Figure 1. The wheel center O is connected to an inertial frame N by springs k_x and k_y and viscous damping elements c_x and c_y to model a suspension system. The displacement of O is expressed as

$$\mathbf{p}^O = x\mathbf{n}_1 + y\mathbf{n}_2, \tag{1}$$

where the unit vectors $\mathbf{n}_1$ and $\mathbf{n}_2$ are fixed in N. The wheel is assumed to be rigid and rotating at a constant angular rate Ω. The tire itself is modelled as an inextensible circular

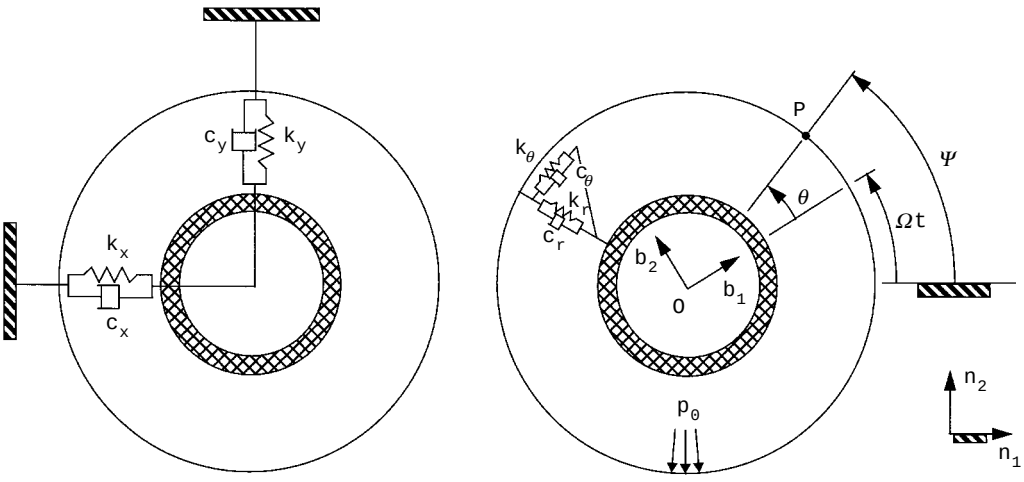

Figure 1. Model of tire–wheel–suspension assembly.

ring on a foundation with distributed spring stiffness k_r and k_θ and damping coefficients, c_r and c_θ in the radial and tangential directions. The nominal mean radius, width, thickness, and density of the ring are denoted by a, b, h, and ρ, respectively. The ring has an internal pressure p_0 and bending stiffness $EI = Db$. Only planar deformations of the ring are considered.

Unit vectors $\mathbf{b}_1$ and $\mathbf{b}_2$ are fixed in the wheel as shown in Figure 1. When the tire is undeformed, the material point P is located at an angle $\theta = \psi - \Omega t$ from $\mathbf{b}_1$ at the mean ring radius. The position vector from O to P at time t is given by

$$\mathbf{p}(\psi, t) = [a + w_r(\psi, t)]\mathbf{d}_r + w_\theta(\psi, t)\mathbf{d}_\theta, \tag{2}$$

where w_r and w_θ are the radial and tangential displacements of P and

$$\mathbf{d}_r = \cos\psi\,\mathbf{n}_1 + \sin\psi\,\mathbf{n}_2, \qquad \mathbf{d}_\theta = \cos\psi\,\mathbf{n}_2 - \sin\psi\,\mathbf{n}_1. \tag{3, 4}$$

Notice from equations (3) and (4) and Figure 1 that $\mathbf{d}_r$ and $\mathbf{d}_\theta$ are radial and tangential directed unit vectors fixed in the inertial frame associated with the angle ψ. The position vector from O to P at time $t + \Delta t$ is given by

$$\mathbf{p}(\psi + \Omega\Delta t, t + \Delta t) = \mathbf{p}(\psi, t) + \frac{\partial \mathbf{p}}{\partial \psi}\Omega\Delta t + \frac{\partial \mathbf{p}}{\partial t}\Delta t + \mathcal{O}(\Delta t^2), \tag{5}$$

where $\mathcal{O}(\Delta t^2)$ denotes second and higher order terms in Δt. Using equations (1)–(5), the velocity of P in N is expressed as

$$\begin{aligned} {}^N\mathbf{v}(\psi, t) &= \dot{x}\mathbf{n}_1 + \dot{y}\mathbf{n}_2 + \lim_{\Delta t \to 0}\{[\mathbf{p}(\psi + \Omega\Delta t, t + \Delta t) - p(\psi, t)]/\Delta t\} \\ &= [\dot{w}_r + \Omega(w_r' - w_\theta) + \dot{x}\cos\psi + \dot{y}\sin\psi]\mathbf{d}_r \\ &\quad + [\dot{w}_\theta + \Omega(a + w_r + w_\theta') - \dot{x}\sin\psi + \dot{y}\cos\psi]\mathbf{d}_\theta, \end{aligned} \tag{6}$$

where the primes and dots denote differentiation with respect to ψ and t, respectively. The velocity of P in the wheel reference frame B is given by

$${}^B\mathbf{v}(\psi, t) = (\dot{w}_r + \Omega w_r')\mathbf{d}_r + (\dot{w}_\theta + \Omega w_\theta')\mathbf{d}_\theta. \tag{7}$$

Equations (6) and (7) are used subsequently to obtain expressions for the kinetic energy of the ring and the virtual work of the foundation damping forces.

For an inextensible ring, the radial and tangential displacements are related by the constraint equation

$$w_r = -w_\theta'. \tag{8}$$

Using equations (6) and (8), the kinetic energy of the ring and wheel is expressed as

$$\begin{aligned} T = \frac{\rho abh}{2}\int_0^{2\pi} &\{[\dot{w}_\theta' + \Omega(w_\theta + w_\theta'') - \dot{x}\cos\psi - \dot{y}\sin\psi]^2 \\ &+ [\dot{w}_\theta + \Omega a - \dot{x}\sin\psi + \dot{y}\cos\psi]^2\}\,\mathrm{d}\psi + [m_w(\dot{x}^2 + \dot{y}^2) + I_w\Omega^2]/2, \end{aligned} \tag{9}$$

where m_w and I_w are the mass and moment of inertia of the wheel. The strain energy of the ring [18], the foundation, and the suspension are given by

$$\begin{aligned} U = \frac{b}{2}\int_0^{2\pi} &\{D(w_\theta' + w_\theta''')^2/a^3 + (\rho ah\Omega^2 + p_0)(w_\theta + w_\theta''')^2 + a[k_\theta w_\theta^2 + k_r(w_\theta')^2]\}\,\mathrm{d}\psi \\ &+ (k_x x^2 + k_y y^2)/2. \end{aligned} \tag{10}$$

Using equations (7) and (8), the virtual work of external forces, damping forces, and the internal pressure [18] is expressed as

$$\delta W = ab \int_0^{2\pi} \{ f_r (\cos\psi \delta x + \sin\psi \delta y - \delta w_\theta') + f_\theta (\cos\psi \delta y - \sin\psi \delta x + \delta w_\theta)$$
$$- c_r (\dot{w}_\theta' + \Omega w_\theta''')\delta w_\theta' - c_\theta (\dot{w}_\theta + \Omega w_\theta')\delta w_\theta + p_0 [-w_\theta' + w_\theta (w_\theta + w_\theta'')/(2a)]\} \, \mathrm{d}\psi$$
$$+ (f_x - c_x \dot{x})\delta x + (f_y - c_y \dot{y})\delta y, \tag{11}$$

where f_r and f_θ are distributed radial and tangential forces acting on the ring and f_x and f_y are forces acting on the wheel in the $\mathbf{n}_1$ and $\mathbf{n}_2$ directions.

Hamilton's principle [19] is written as

$$\int_{t_1}^{t_2} (\delta T - \delta U + \delta W) \, \mathrm{d}t = 0, \tag{12}$$

where δ is the vibrational symbol. Substituting equations (9)–(11) into equation (12), integrating by parts, and setting the coefficients of δw_θ, δx, and δy equal to zero yields the following equations of motion:

$$\rho h[\ddot{w}_\theta - \ddot{w}_\theta'' - 2\ddot{x}\sin\psi + 2\ddot{y}\cos\psi - 2\Omega(\dot{w}_\theta' + \dot{w}_\theta''')] + L_\theta = d_\theta + f_r', \tag{13}$$

$$(m_w + m_r)\ddot{x} + c_x \dot{x} + k_x x + L_x = f_x + ab \int_0^{2\pi} (f_r \cos\psi - f_\theta \sin\omega) \, \mathrm{d}\psi, \tag{14}$$

$$(m_w + m_r)\ddot{y} + c_y \dot{y} + k_y y + L_y = f_y + ab \int_0^{2\pi} (f_\theta \cos\psi + f_r \sin\psi) \, \mathrm{d}\psi, \tag{15}$$

where

$$L_\theta = -D(w_\theta'' + 2w_\theta^{IV} + w_\theta^{VI})/a^4 + p_0 (w_\theta'' + w_\theta^{IV})/a - k_r w_\theta'' + k_\theta w_\theta$$
$$- c_r (\dot{w}_\theta'' + \Omega w_\theta''') + c_\theta (\dot{w}_\theta + \Omega w_\theta'), \tag{16}$$

$$L_x = -\rho abh \int_0^{2\pi} \{\cos\psi[\ddot{w}_\theta' + \Omega(\dot{w}_\theta + \dot{w}_\theta'')] + \ddot{w}_\theta \sin\psi\} \, \mathrm{d}\psi, \tag{17}$$

$$L_y = -\rho abh \int_0^{2\pi} \{\sin\psi[\ddot{w}_\theta' + \Omega(\dot{w}_\theta + \dot{w}_\theta'')] - \ddot{w}_\theta \cos\psi\} \, \mathrm{d}\psi, \tag{18}$$

$$m_r = 2\pi\rho abh. \tag{19}$$

The undamped natural frequencies of the system can be determined by setting the damping coefficients and forcing terms in equations (13)–(15) equal to zero and assuming a solution of the form

$$w_\theta(\psi, t) = a_0 \cos\omega_0 t + (a_1 \cos\psi + b_1 \sin\psi)\cos\omega_1 t + \sum_{n=2}^{\infty} a_n \cos(n\psi + \omega_n t), \tag{20}$$

$$x = x_1 \cos\omega_1 t, \qquad y = y_1 \cos\omega_1 t. \tag{21, 22}$$

The assumed form of the solution used in the summation of equation (20) reflects the fact that the mode shapes for $n > 1$ are complex. That is, the maximum deformation of all points on the tire is not reached at the same time.

The natural frequencies ω_1 are the solutions to either of the characteristic equations

$$m_r m_w \omega_1^4 - [\pi ab(k_r + k_\theta)(m_w + m_r) - k_x m_r]\omega_1^2 + \pi ab(k_r + k_\theta)k_x = 0,$$
$$m_r m_w \omega_1^4 - [\pi ab(k_r + k_\theta)(m_w + m_r) - k_y m_r]\omega_1^2 + \pi ab(k_r + k_\theta)k_y = 0. \quad (23)$$

For $n \neq 1$, one obtains

$$\omega_n = -\frac{\Omega n(n^2 - 1)}{n^2 + 1} \pm \sqrt{\frac{\Omega^2 n^2 (n^2 - 1)^2}{(n^2 + 1)^2} + \hat{\omega}_n^2}, \quad (24)$$

where

$$\hat{\omega}_n^2 = [Dn^2(n^2 - 1)^2/a^4 + p_0 n^2(n^2 - 1)/a + k_\theta + n^2 k_r]/[\rho h(n^2 + 1)]. \quad (25)$$

The mode shapes of the system not in ground contact can be interpreted as deformation patterns given by $\cos n\psi$ traveling in the clockwise direction at the angular rate ω_n / n. In order to relate the natural frequencies in the fixed reference frame to those observed in the wheel reference frame B, the angle θ defined by $\theta = \psi - \Omega t$ is introduced. Notice that a fixed value of θ corresponds to a particular material point on the ring. By substituting $\psi = \theta + \Omega t$ into the expression $\cos(n\psi + \omega_n t)$, one observes that the coefficient of t is $\omega_n + n\Omega$. Thus, the natural frequencies of vibration in the wheel reference frame differ from ω_n by the rotation rate multiplied by the wave number. Adding Ωn to the right hand side of equation (24) yields

$${}^B\omega_n = \frac{2\Omega n}{n^2 + 1} \pm \sqrt{\frac{\Omega^2 n^2 (n^2 - 1)^2}{(n^2 + 1)^2} + \hat{\omega}_n^2}. \quad (26)$$

The natural frequencies of the system in the wheel reference frame given by equation (26) are consistent with previous results [20] in which the equations of motion were formulated in a rotating rather than a fixed reference frame.

For purposes of comparison, the external buckling pressure for a stationary ring is determined by setting $\hat{\omega}_n$ equal to zero in equation (25) and solving for $p_n = -p_0$. The result is

$$p_n = \frac{D(n^2 - 1)}{a^3} + \frac{(k_\theta + n^2 k_r)a}{n^2(n^2 - 1)}. \quad (27)$$

The critical buckling pressure given by equation (27) is consistent with previous results [18] in which the tangential foundation stiffness is set equal to zero.

In order to obtain solutions to equations (13)–(15), the functions w_θ and $f_\theta + f_r'$ are expanded as Fourier series:

$$w_\theta(\psi, t) = \alpha_0(t)/2 + \sum_{n=1}^{\infty} [\alpha_n(t)\cos n\psi + \beta_n(t)\sin n\psi], \quad (28)$$

$$f_\theta + f_r' = g_0(t)/2 + \sum_{n=1}^{\infty} [g_n(t)\cos n\psi + h_n(t)\sin n\psi], \quad (29)$$

where

$$g_n = \frac{1}{\pi}\int_0^{2\pi} (f_\theta \cos n\psi + nf_r \sin n\psi)\, \mathrm{d}\psi, \tag{30}$$

$$h_n = \frac{1}{\pi}\int_0^{2\pi} (f_\theta \sin n\psi - nf_r \cos n\psi)\, \mathrm{d}\psi. \tag{31}$$

Substituting equations (28) and (29) into equations (13)–(18) and equating coefficients of the $\cos n\psi$ and $\sin n\psi$ terms yields

$n = 0$:

$$\rho h\ddot{\alpha}_0 + c_\theta \dot{\alpha}_0 + k_\theta \alpha_0 = g_0\,; \tag{32}$$

$n = 1$:

$$2\rho h \begin{bmatrix} 1 & 0 & 0 & 1 \\ 0 & 1 & -1 & 0 \\ 0 & -1 & \gamma & 0 \\ 1 & 0 & 0 & \gamma \end{bmatrix} \begin{bmatrix} \ddot{\alpha}_1 \\ \ddot{\beta}_1 \\ \ddot{x} \\ \ddot{y} \end{bmatrix} + \begin{bmatrix} c_1 & 0 & 0 & 0 \\ 0 & c_1 & 0 & 0 \\ 0 & 0 & \frac{c_x}{\pi ab} & 0 \\ 0 & 0 & 0 & \frac{c_y}{\pi ab} \end{bmatrix} \begin{bmatrix} \dot{\alpha}_1 \\ \dot{\beta}_1 \\ \dot{x} \\ \dot{y} \end{bmatrix}$$

$$+ \begin{bmatrix} k_1 & \Omega c_1 & 0 & 0 \\ -\Omega c_1 & k_1 & 0 & 0 \\ 0 & 0 & \frac{k_z}{\pi ab} & 0 \\ 0 & 0 & 0 & \frac{k_y}{\pi ab} \end{bmatrix} \begin{bmatrix} \alpha_1 \\ \beta_1 \\ x \\ y \end{bmatrix} + \begin{bmatrix} g_1 \\ h_1 \\ f_x/(\pi ab) + \frac{1}{\pi}\int_0^{2\pi} (f_r \cos\psi - f_\theta \sin\psi)\, \mathrm{d}\psi \\ f_y/(\pi ab) + \frac{1}{\pi}\int_0^{2\pi} (f_\theta \cos\psi + f_r \sin\psi)\, \mathrm{d}\psi \end{bmatrix}; \tag{33}$$

$n > 1$:

$$\rho h(n^2+1)\begin{bmatrix} \ddot{\alpha}_n \\ \ddot{\beta}_n \end{bmatrix} + \begin{bmatrix} c_n & 2\rho h\Omega n(n^2-1) \\ -2\rho h\Omega n(n^2-1) & c_n \end{bmatrix}\begin{bmatrix} \dot{\alpha}_n \\ \dot{\beta}_n \end{bmatrix}$$

$$+ \begin{bmatrix} k_n & \Omega n c_n \\ -\Omega n c_n & k_n \end{bmatrix}\begin{bmatrix} \alpha_n \\ \beta_n \end{bmatrix} = \begin{bmatrix} g_n \\ h_n \end{bmatrix}; \tag{34}$$

where

$$\gamma = 1 + m_w/m_r, \qquad c_n = n^2 c_r + c_\theta, \tag{35, 36}$$

$$k_n = Dn^2(n^2-1)^2/a^4 + p_0\, n^2(n^2-1)/a + k_\theta + n^2 k_r. \tag{37}$$

It is evident from equations (32)–(34) that coupling of the wheel d.o.f. (x and y) only occurs with the rigid body translation modes of the tire ($n = 1$). Moreover, the equations of motion are time-invariant. That is, the coefficient matrices appearing in equations (32)–(34) are all constant.

A simple eigenvalue analysis reveals that the null solutions to equations (32) and (34) in the absence of forcing terms are asymptotically stable provided that all the damping and stiffness parameters are positive. The steady-state solution to these equations for constant values of g_n and h_n are given by

$$\alpha_n = (k_n g_n - \Omega n c_n h_n)/(k_n^2 + \Omega^2 n^2 c_n^2), \tag{38}$$

$$\beta_n = (k_n h_n + \Omega n c_n g_n)/(k_n^2 + \Omega^2 n^2 c_n^2). \tag{39}$$

Notice that the response predicted by equations (38) and (39) is always bounded regardless of the value of Ω. Thus, for a constant stationary load, there is no critical value of Ω for $n \neq 1$. The same observation was made previously [2] for a similar tire model.

A noteworthy feature of equation (33) is that the coefficient matrices are all constant. This feature is not present in a related study [15] where a coupled system with periodic coefficients is obtained. In that study, a Floquet analysis requiring numerical time integration of the equations of motion was used to determine the stability of the unforced system. In contrast, the present study only requires an eigenvalue analysis of equation (33) to determine stability. Although direct comparison of the two studies is not readily accomplished because of some modelling differences, one can show that the time-varying system of the cited reference can be transformed to an equivalent time-invariant system via the transformation of variables

$$\alpha_1 = \tilde{\alpha}_1 \cos \Omega t + \tilde{\beta}_1 \sin \Omega t, \qquad \beta_1 = \tilde{\beta}_1 \cos \Omega t - \tilde{\alpha}_1 \sin \Omega t. \tag{40, 41}$$

Indeed, substitution of equations (40) and (41) into equation (4.6) of reference [15] leads to the time-invariant system

$$\begin{bmatrix} \ddot{\tilde{\alpha}}_1 \\ \ddot{\tilde{\beta}}_1 \\ \ddot{y} \end{bmatrix} + \begin{bmatrix} \frac{\lambda_1}{\rho h} & 0 & 0 \\ 0 & \frac{\lambda_1}{\rho h} & 0 \\ 0 & 0 & \frac{c_s}{M} \end{bmatrix} \begin{bmatrix} \dot{\tilde{\alpha}}_1 \\ \dot{\tilde{\beta}}_1 \\ \dot{y} \end{bmatrix}$$

$$+ \begin{bmatrix} \frac{k_z + k_\theta}{2\rho h} & \frac{\lambda_1 \Omega}{\rho h} & 0 \\ -\frac{\lambda_1 \Omega}{\rho h} & \frac{k_z + k_\theta}{2\rho h} & -\frac{k_z + k_\theta}{2\rho h} \\ 0 & -\frac{ab\pi(k_z + k_\theta)}{M} & \frac{ab\pi(k_z + k_\theta)}{M} + \frac{k_s}{M} \end{bmatrix} \begin{bmatrix} \tilde{\alpha}_1 \\ \tilde{\beta}_1 \\ y \end{bmatrix} = \begin{bmatrix} -F \\ 0 \\ 0 \end{bmatrix}. \tag{42}$$

3. STATIC RESPONSE OF CONTACTING TIRE

The governing equations are now used to determine the static response of a rotating tire in contact with a flat frictionless surface. As an approximation, the function w_θ is expressed as a truncated Fourier series:

$$w_\theta(\psi) = \alpha_0/2 + \sum_{n=1}^{M} \alpha_n \cos n\psi + \beta_n \sin n\psi. \tag{43}$$

The assumption of a frictionless surface implies that the contact forces acting on the tire are in the vertical direction alone. Thus, the radial and tangential forces are given by

$$f_r(\psi) = f(\psi)\sin\psi, \qquad f_\theta(\psi) = f(\psi)\cos\psi, \tag{44, 45}$$

where f is the contact force. Consistent with the use of equation (43), one can verify that the ring model of the tire only contacts the flat surface at a finite number of angular locations. Thus, the contact force can be expressed as

$$f(\psi) = \sum_{j=1}^{p} f_{cj}\,\delta(\psi - \psi_{cj}), \tag{46}$$

where p is the number of contact locations, δ denotes the Dirac delta function and ψ_{cj} is the jth angular location where contact occurs. In order to solve the contact problem, one must determine the contact locations and forces as well as their number p.

The number of contact locations p depends on the ring and foundation stiffnesses, the load supported by the suspension F, and the number of harmonics M used in equation (43). In general, p increases for increasing values of F and M and decreases for increasing values of the ring and foundation stiffnesses. For the problems considered in this study, contact occurs at four locations. In the limit as $M \to \infty$, the tire contacts the surface along a line (or lines) rather than at discrete locations.

It is assumed that the bottom of the tire is in imminent contact under a zero load condition. Contact is accomplished by vertically displacing the flat surface by an amount z such that a net vertical load F is supported by the suspension. Force equilibrium in the vertical direction and contact at the angular locations ψ_{cj} imply that

$$\sum_{j=1}^{p} f_{cj} = F/(ab), \qquad r(\psi_{cj}) = r(\psi_{c,j+1}), \qquad (j = 1, \ldots, p-1), \tag{47, 48}$$

where $r(\psi)$ denotes the vertical position of the ring at the angular location ψ due to concentrated forces at the angular locations ψ_{cj}. Using the inextensibility assumption of equation (8), one obtains

$$r(\psi) = y + [a - w'_\theta(\psi)]\sin\psi + w_\theta(\psi)\cos\psi. \tag{49}$$

At the points of contact, the derivative of r with respect to ψ must equal zero. Thus,

$$r'(\psi_{cj}) = 0 \qquad (j = 1, \ldots, p). \tag{50}$$

Setting all the dotted terms in equations (32)–(34) equal to zero and making use of equations (30, 31) and (44)–(47) yields

$$x = 0, \qquad y = F/k_y, \qquad \alpha_0 = g_0/k_\theta, \qquad \begin{bmatrix}\alpha_n \\ \beta_n\end{bmatrix} = \begin{bmatrix} k_n & \Omega n c_n \\ -\Omega n c_n & k_n\end{bmatrix}^{-1}\begin{bmatrix} g_n \\ h_n\end{bmatrix}, \tag{51–54}$$

where

$$g_n = \sum_{j=1}^{p} f_{cj}\,(\cos n\psi_{cj}\cos\psi_{cj} + n\sin n\psi_{cj}\sin\psi_{cj})/\pi, \tag{55}$$

$$h_n = \sum_{j=1}^{p} f_{cj}\,(\sin n\psi_{cj}\cos\psi_{cj} - n\cos n\psi_{cj}\sin\psi_{cj})/\pi. \tag{56}$$

TABLE 1

System parameter values used in examples

Parameter	Value
ρ	1590 kg/m^3
a	0·305 m
b	0·152 m
h	0·0127 m
D	21·75 Nm
k_r	$5{\cdot}80 \times 10^6$ N/m^3
k_θ	$4{\cdot}03 \times 10^6$ N/m^3
p_0	$2{\cdot}07 \times 10^5$ N/m^2
k_y	$3{\cdot}60 \times 10^4$ N/m
F	1960 N

Substituting equation (43) into equation (49), one obtains

$$r(\psi) = y + a\sin\psi + \frac{\alpha_0}{2}\cos\psi + \sum_{n=1}^{M}[\alpha_n(\cos n\psi\cos\psi + n\sin n\psi\sin\psi) + \beta_n(\sin n\psi\cos\psi - n\cos n\psi\sin\psi)]. \quad (57)$$

Differentiating equation (57) with respect to ψ yields

$$r'(\psi) = a\cos\psi - \frac{\alpha_0}{2}\sin\psi + \sum_{n=1}^{M}(n^2-1)(\alpha_n\cos n\psi\sin\psi + \beta_n\sin n\psi\sin\psi), \quad (58)$$

$$r''(\psi) = -a\sin\psi - \frac{\alpha_0}{2}\cos\psi + \sum_{n=1}^{M}(n^2-1)[\alpha_n(\cos n\psi\cos\psi - n\sin n\psi\sin\psi) + \beta_n(\sin n\psi\cos\psi + n\cos n\psi\sin\psi)]. \quad (59)$$

It is evident that constraint equations (48) and (50) can be expressed solely in terms of the unknowns f_{cj} and ψ_{cj} by making use of equations (53)–(58). Thus, equations (47, 48) and (50) comprise a set of $2p$ equations in $2p$ unknowns. Because the constraint equations are non-linear, a numerical approach is generally required in order to obtain a solution. The exception is for cases in which there is only one contact location and the tire is either stationary ($\Omega = 0$) or the damping coefficients c_r and c_θ are both zero. For these cases, the solution is given simply by $f_{c1} = F/(ab)$ and $\psi_{c1} = -\pi/2$. For all other cases, Newton's method is used to obtain the solution. After the solution is obtained, r'' is calculated at the contact locations from equation (59). Positive values of $r''(\psi_{cj})$ and f_{cj} together with a plot of the deformed shape of the ring are used to verify the assumption that contact occurs at p locations.

To illustrate the effects of rotation and damping on the static response, consider a system with the properties given in Table 1. These properties are identical to the ones used in reference [15]. The damping coefficients c_θ and c_r are given by

$$c_\theta = 2\zeta_0\sqrt{k_\theta\rho h}, \qquad c_r = 2\zeta_1\sqrt{2(k_r + k_\theta)\rho h} - c_\theta, \quad (60, 61)$$

where ζ_0 and ζ_1 are the damping ratios of the $n = 0$ and $n = 1$ modes for a fixed wheel and unconstrained tire. For the results presented, ζ_0 and ζ_1 are both set equal to ζ and $M = 400$. The suspension damping coefficients have no effect on the static response.

Plots of the deformed shape of the tire near the points of contact are shown in Figure 2 for three different values of $\Omega\zeta$. Notice that the contact locations move to the left for

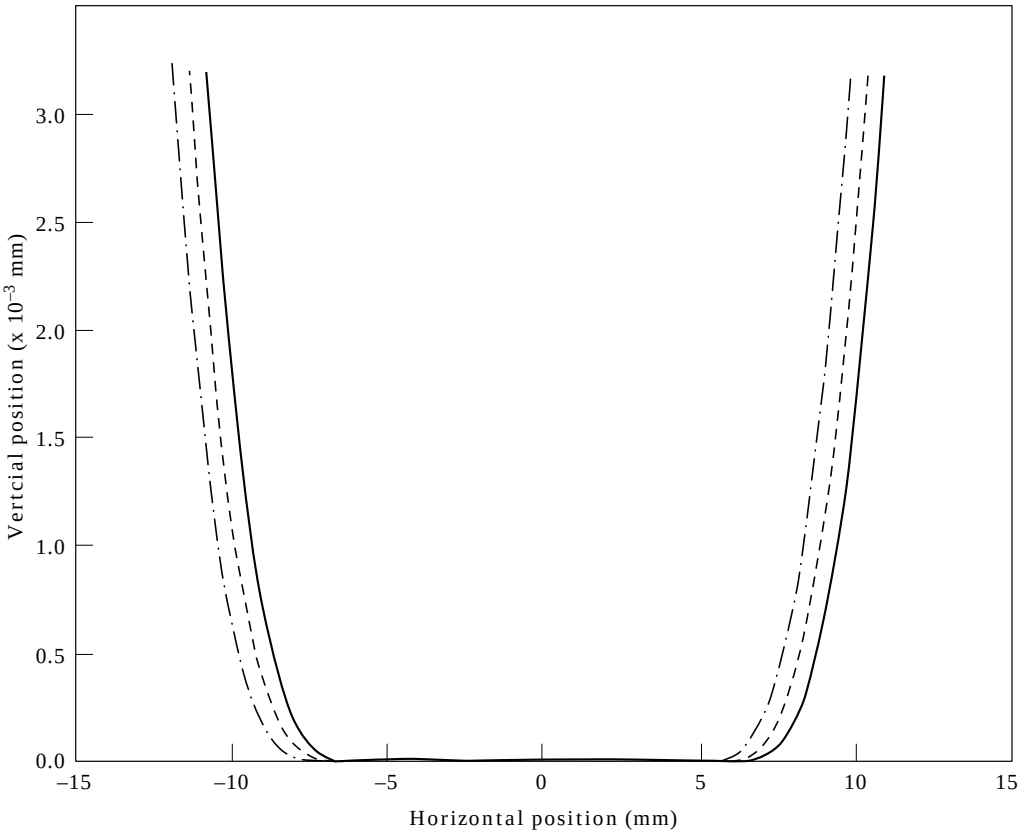

Figure 2. Deformed shape of tire near contact area (——, $\Omega n = 0$; – – –, $\Omega n = 5$; –·–, $\Omega n = 10$).

increasing values of $\Omega\zeta$. This observation is consistent with the fact that a positive moment must be applied to the wheel in order to maintain a constant rate of rotation. The rate of work done by the applied moment equals the rate of energy dissipation caused by damping in the tire.

To illustrate the effects of damping and rotation on the rolling resistance, let M_f denote the net moment of the contact forces about the wheel center. The frictional coefficient μ_r is then defined as

$$\mu_r = M_f /(Fa) \tag{62}$$

A plot of μ_r versus $\Omega\zeta$ is shown in Figure 3. Notice that the curve is well-approximated by a linear function of $\Omega\zeta$.

4. MODAL CHARACTERISTICS OF CONTACTING TIRE

In the following development, terms with an overhat refer to specific values associated with the static equilibrium. Perturbation variables $\tilde{\alpha}_n$, $\tilde{\beta}_n$, $\tilde{y}$, $\tilde{f}_{cj}$ and $\tilde{\psi}_{cj}$ are defined as

$$\tilde{\alpha}_n = \alpha_n - \hat{\alpha}_n, \qquad \tilde{\beta}_n = \beta_n - \hat{\beta}_n, \qquad \tilde{y} = y - \hat{y}, \tag{63–65}$$

$$\tilde{f}_{cj} = f_{cj} - \hat{f}_{cj}, \qquad \tilde{\psi}_{cj} = \psi_{cj} - \hat{\psi}_{cj}. \tag{66, 67}$$

Setting the applied wheel forces f_x and f_y equal to zero and linearizing the right hand sides of equations (32)–(34) about the static equilibrium yields

$n = 0$:

$$(\rho h \ddot{\tilde{\alpha}}_0 + c_\theta \dot{\tilde{\alpha}}_0 + k_\theta \tilde{\alpha}_0)/2 = (b_{01}^T \tilde{f}_c + b_{03}^T \hat{F}_c \tilde{\psi}_c)/(2\pi); \tag{68}$$

$n = 1$:

$$2\rho h \begin{bmatrix} 1 & 0 & 0 & 1 \\ 0 & 1 & -1 & 0 \\ 0 & -1 & \gamma & 0 \\ 1 & 0 & 0 & \gamma \end{bmatrix} \begin{bmatrix} \ddot{\tilde{\alpha}}_1 \\ \ddot{\tilde{\beta}}_1 \\ \ddot{x} \\ \ddot{y} \end{bmatrix} + \begin{bmatrix} c_1 & 0 & 0 & 0 \\ 0 & c_1 & 0 & 0 \\ 0 & 0 & \frac{c_x}{\pi ab} & 0 \\ 0 & 0 & 0 & \frac{c_y}{\pi ab} \end{bmatrix} \begin{bmatrix} \dot{\tilde{\alpha}}_1 \\ \dot{\tilde{\beta}}_1 \\ \dot{x} \\ \dot{y} \end{bmatrix}$$

$$+ \begin{bmatrix} k_1 & \Omega c_1 & 0 & 0 \\ -\Omega c_1 & k_1 & 0 & 0 \\ 0 & 0 & \frac{k_x}{\pi ab} & 0 \\ 0 & 0 & 0 & \frac{k_y}{\pi ab} \end{bmatrix} \begin{bmatrix} \tilde{\alpha}_1 \\ \tilde{\beta}_1 \\ x \\ \tilde{y} \end{bmatrix} = \begin{bmatrix} b_{11}^T \tilde{f}_c / \pi \\ 0 \\ 0 \\ b_{11}^T \tilde{f}_c / \pi \end{bmatrix}; \tag{69}$$

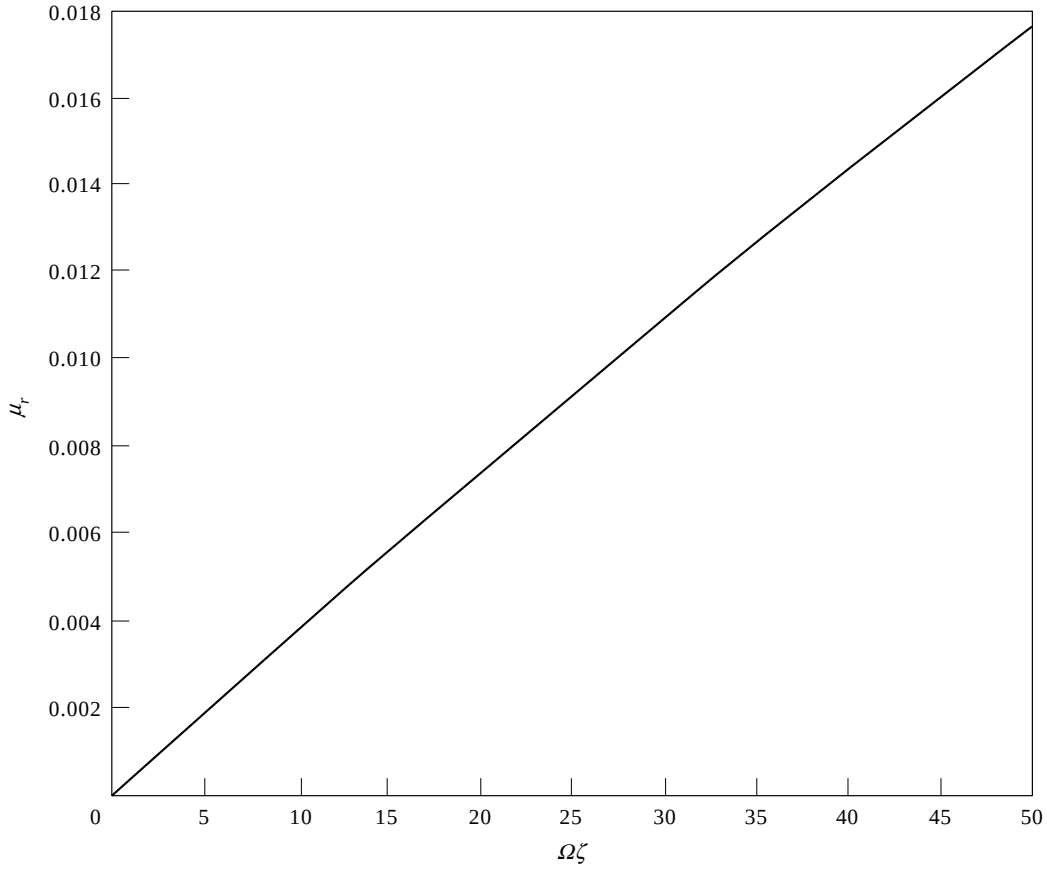

Figure 3. Frictional coefficient μ_r as a function of $\Omega\zeta$.

$n > 1$:

$$\rho h(n^2+1)\begin{bmatrix}\ddot{\tilde{\alpha}}_n\\ \ddot{\tilde{\beta}}_n\end{bmatrix}+\begin{bmatrix}c_n & 2\rho h\Omega n(n^2-1)\\ -2\rho h\Omega n(n^2-1) & c_n\end{bmatrix}\begin{bmatrix}\dot{\tilde{\alpha}}_n\\ \dot{\tilde{\beta}}_n\end{bmatrix}$$

$$+\begin{bmatrix}k_n & \Omega n c_n\\ -\Omega n c_n & k_n\end{bmatrix}\begin{bmatrix}\tilde{\alpha}_n\\ \tilde{\beta}_n\end{bmatrix}=\frac{1}{\pi}\begin{bmatrix}b_{n1}^T\tilde{f}_c+b_{n3}^T\hat{F}_c\tilde{\psi}_c\\ b_{n2}^T\tilde{f}_c+b_{n4}^T\hat{F}_c\tilde{\psi}_c\end{bmatrix}; \quad (70)$$

where

$$\tilde{f}_c=[\tilde{f}_{c1}\cdots\tilde{f}_{cp}]^T, \qquad \tilde{\psi}_c=[\tilde{\psi}_{c1}\cdots\tilde{\psi}_{cp}]^T, \qquad \hat{F}_c=\text{diag}\,[\hat{f}_{c1},\ldots,\hat{f}_{cp}] \quad (71\text{–}73)$$

and the jth elements of $b_{n1},\ldots,b_{n4}$ are given by

$$b_{n1}(j)=\cos n\hat{\psi}_{cj}\cos\hat{\psi}_{cj}+n\sin n\hat{\psi}_{cj}\sin\hat{\psi}_{cj}, \quad (74)$$

$$b_{n2}(j)=\sin n\hat{\psi}_{cj}\cos\hat{\psi}_{cj}-n\cos n\hat{\psi}_{cj}\sin\hat{\psi}_{cj}, \quad (75)$$

$$b_{n3}(j)=(n^2-1)\cos n\hat{\psi}_{cj}\sin\hat{\psi}_{cj}, \qquad b_{n4}(j)=(n^2-1)\sin n\hat{\psi}_c\sin\hat{\psi}_{cj}. \quad (76,77)$$

Linearizing the contact boundary conditions $r(\psi_{cj})=r(\hat{\psi}_{cj})$ and $r'(\psi_{cj})=0$ for $j=1,\ldots,p$ about the static equilibrium yields

$$A_1^T q=0, \qquad C\tilde{\psi}_c+A_2^T q=0, \quad (78,79)$$

where

$$A_1=[b_{01}/2 \quad b_{11} \quad b_{12} \quad \cdots \quad b_{M1} \quad b_{M2} \quad 0 \quad b_{11}]^T, \quad (80)$$

$$A_2=[b_{03}/2 \quad b_{13} \quad b_{14} \quad \cdots \quad b_{M3} \quad b_{M4} \quad 0 \quad 0]^T, \quad (81)$$

$$C=\text{diag}\,[r''(\hat{\psi}_{c1}),\ldots,r''(\hat{\psi}_{cp})], \quad (82)$$

$$q=[\tilde{\alpha}_0 \quad \tilde{\alpha}_1 \quad \tilde{\beta}_1 \quad \cdots \quad \tilde{\alpha}_M \quad \tilde{\beta}_M \quad x \quad y]^T. \quad (83)$$

Equations (68)–(70) can be expressed equivalently as

$$\bar{M}\ddot{q}+\bar{C}\dot{q}+\bar{K}q=(A_1\tilde{f}_c+A_2\hat{F}_c\tilde{\psi}_c)/\pi, \quad (84)$$

where the elements of $\bar{M}$, $\bar{C}$, $\bar{K}$ are given in the Appendix. Combining equations (78, 79) and (84), one obtains

$$\begin{bmatrix}\bar{M} & 0 & 0\\ 0 & 0 & 0\\ 0 & 0 & 0\end{bmatrix}\begin{bmatrix}\ddot{q}\\ \ddot{\tilde{f}}_c\\ \ddot{\tilde{\psi}}_c\end{bmatrix}+\begin{bmatrix}\bar{C} & 0 & 0\\ 0 & 0 & 0\\ 0 & 0 & 0\end{bmatrix}\begin{bmatrix}\dot{q}\\ \dot{\tilde{f}}_c\\ \dot{\tilde{\psi}}_c\end{bmatrix}+\begin{bmatrix}\bar{K} & -A_1/\pi & -A_2\hat{F}_c/\pi\\ A_1^T & 0 & 0\\ A_2^T & 0 & C\end{bmatrix}\begin{bmatrix}q\\ \tilde{f}_c\\ \tilde{\psi}_c\end{bmatrix}=\begin{bmatrix}0\\ 0\\ 0\end{bmatrix}. \quad (85)$$

The mode shapes and frequencies of the system can now be determined by transforming equation (85) to an equivalent first-order form and solving the associated eigenvalue problem.

The damping coefficients c_x and c_y can be expressed in terms of the suspension damping ratios ζ_x and ζ_y as

$$c_x=2\zeta_x\sqrt{k_x(m_w+m_r)}, \qquad c_y=2\zeta_y\sqrt{k_y(m_w+m_r)}. \quad (86,87)$$

For the results presented, ζ_x and ζ_y are both set equal to ζ_s.

The first ten mode shapes and natural frequencies in Hertz of the undamped system in ground contact for $\Omega = 0$ are shown in Figure 4 for $k_x = 1000k_y$. The dashed lines and circles in the figure correspond to the static deformation of the tire and wheel center, whereas the solid lines and x's are associated with the mode shapes. Notice that there is little horizontal motion of the wheel center for any of the modes because of the large horizontal suspension stiffness.

A one-to-one correspondence between the mode shapes of the system not in ground contact can be made with those in Figure 4. Modes (a) and (c) can be paired with $n = 1$ harmonics, whereas the torsional Mode (b) is associated with the $n = 0$ harmonic. Modes (d) and (e), (f) and (g), (h) and (i), and (j) are associated with the $n = 2$, $n = 3$, $n = 4$, and $n = 5$ harmonics, respectively.

The frequencies and damping ratios of the system in ground contact as a function of Ω are shown in Figures 5 and 6, respectively. These results were obtained by setting $\zeta_s = 0{\cdot}05$ and $\zeta = 0{\cdot}04$. The results shown were calculated by solving the first-order form of the eigenvalue problem associated with equation (85) using an Arnoldi method [21].

The frequencies of the first three modes appear to be relatively insensitive to changes in the rotation rate. In contrast, the frequencies of Modes (d)–(j) all have a noticeable dependence on Ω. The damping ratios of Modes (b) and (c) are nearly independent of Ω. The most significant effects of the rotation rate on the damping ratios occurs for Modes (d)–(f) and (h).

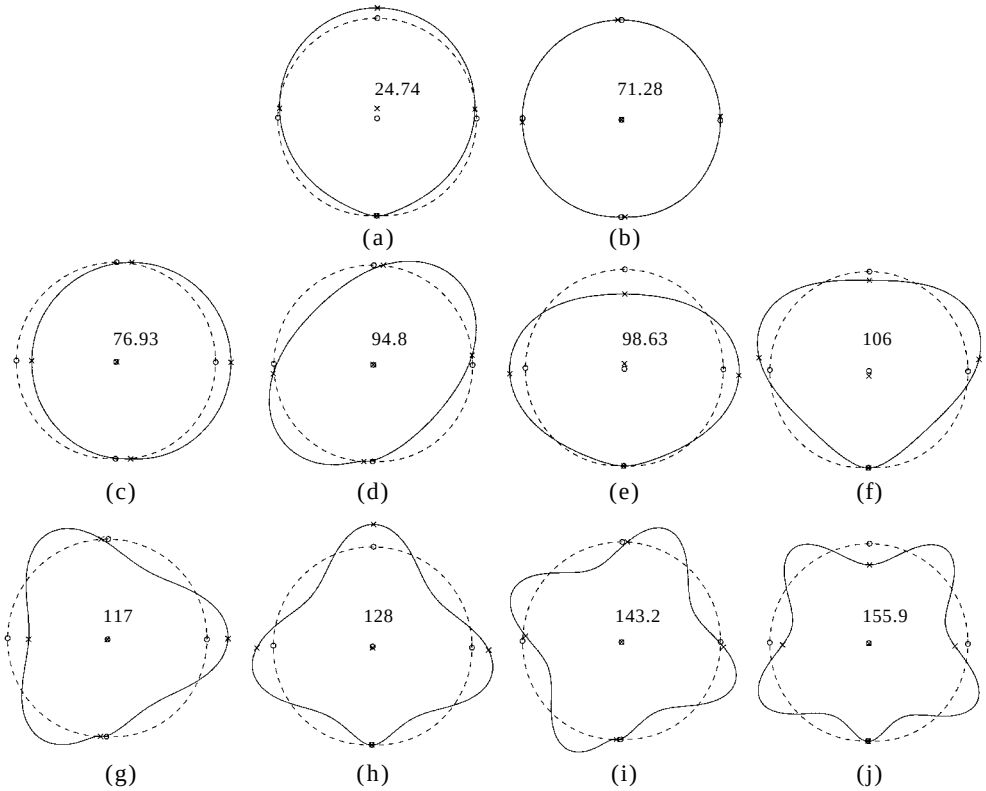

Figure 4. First ten mode shapes and frequencies (Hz) of undamped system in ground contact. Designations are: (a) 1st vertical; (b) torsional; (c) fore-aft; (d) $n = 2$; (e) 2nd vertical; (f) 3rd vertical; (g) $n = 3$; (h) 4th vertical; (i) $n = 4$; and (j) 5th vertical.

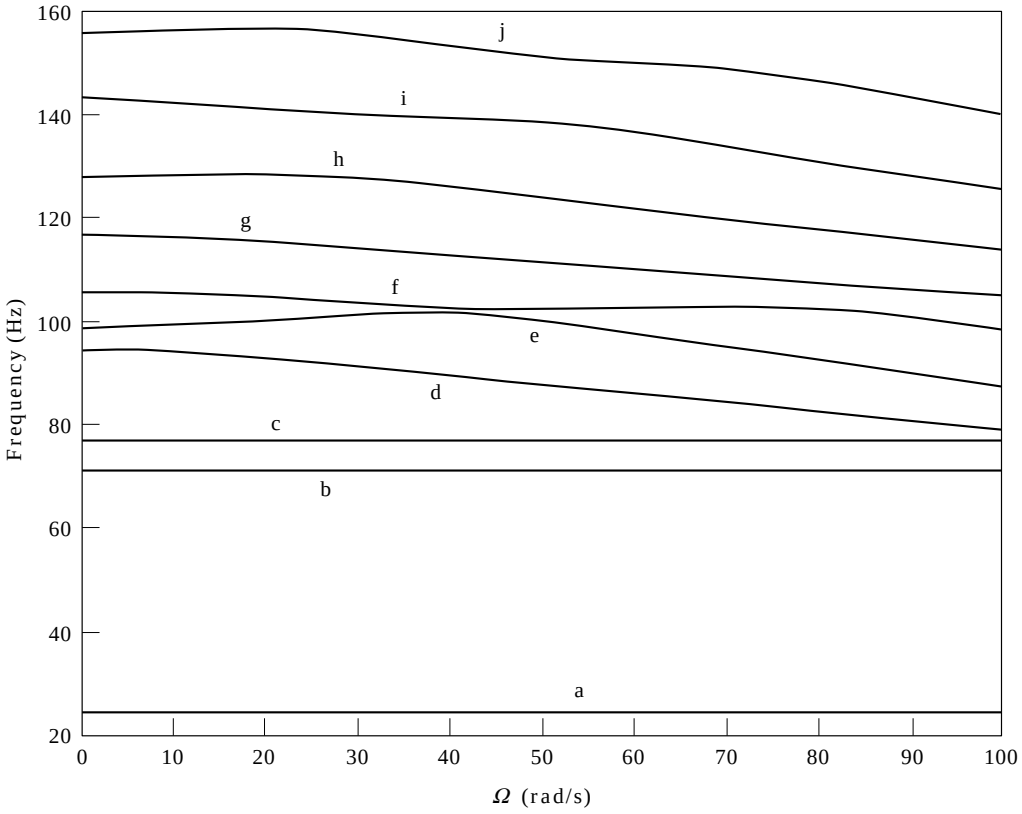

Figure 5. Natural frequencies of damped system in ground contact versus Ω.

5. CONCLUSIONS

The derivation presented in section 2 shows that the equations of motion for the tire–wheel–suspension assembly can be expressed as a linear, time-invariant system. This result is contrasted by previously published work [15] in which a parametrically excited system with periodic coefficients is obtained. The time-invariance of the governing equations follows from expressing tire deformations as functions of a fixed-frame rather than a rotating-frame co-ordinate. With such an approach, the determination of stability, static deformation, and modal characteristics of the system in ground contact is simplified significantly.

A method was developed to determine the static deformation of a vertically loaded tire in contact with a flat and frictionless surface. As expected, non-zero values of damping and rotation caused the contact patch for the tire to shift in the direction of motion. The frictional coefficient for rolling was shown to be well approximated by a linear function of the product of the rotation rate and a damping ratio associated with energy dissipation of the tire.

A method was developed to determine the frequencies, mode shapes, and damping ratios of a rotating tire in ground contact. The frequencies of the first three modes of the system were relatively insensitive to changes in the rotation rate while the remaining seven modes tracked showed a measurable change in frequency. The damping ratios of the second and third modes of the system were nearly independent of the rotation rate. The most

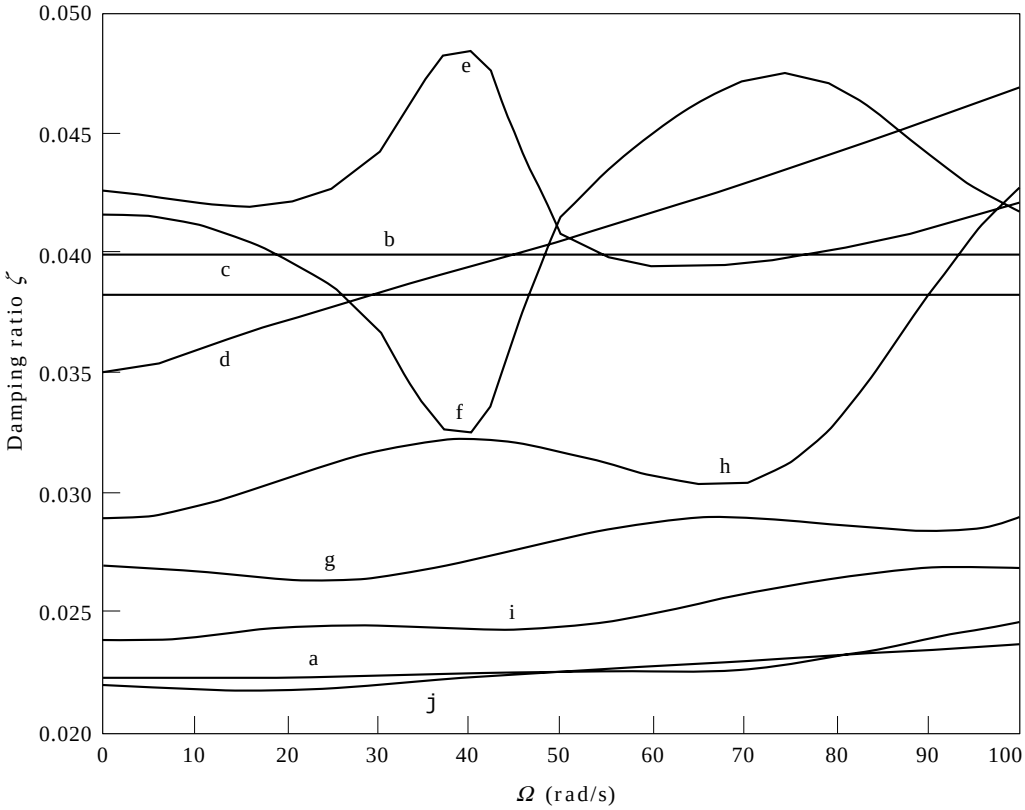

Figure 6. Damping ratios of system in ground contact versus Ω.

significant effects of rotation on the damping ratios occurred for the fourth through sixth and eighth modes of the system.

ACKNOWLEDGMENT

This work, performed at Sandia National Laboratories, was supported by the U.S. Department of Energy under contract DE-AC04-94AL85000.

REFERENCES

1. G. R. Potts, C. A. Bell, L. T. Charek and T. K. Roy 1978 *Tire Science and Technology* **5**, 202–225. Tire vibrations.
2. S. C. Huang and W. Soedel 1987 *Journal of Sound and Vibration* **115**, 253–274. Effects of Coriolis acceleration on the free and force in-plane vibrations of rotating rings on elastic foundation.
3. S. C. Huang and W. Soedel 1987 *Journal of Sound and Vibration* **118**, 253–270. Response of rotating rings to harmonic and periodic loading and comparison with the inverted problem.
4. S. Gong 1993 *Doctorate Thesis*, *Delft University of Technology*, A study of in-plane dynamics of tires.
5. S. C. Huang and C. K. Su 1992 *Vehicle System Dynamics* **21**, 247–267. In-plane dynamics of tires on the road based on an experimentally verified rolling ring model.
6. W. Soedel 1975 *Journal of Sound and Vibration* **41**, 233–246. On the dynamic response of rolling tires according to thin shell approximations.

7. W. Soedel and M. G. Prasad 1980 *Journal of Sound and Vibration* **70**, 573–584. Calculation of natural frequencies and modes of tires in road contact by utilizing eigenvalues of the axisymmetric non-contacting tire.
8. T. R. Richards, J. E. Brown, R. L. Hohman and S. V. Sundaram 1985 *Third International Modal Analysis Conference*, 857–863. Modal analysis of tires relevant to vehicle system dynamics.
9. L. E. Kung, W. Soedel, T. Y. Yang and L. T. Charek 1985 *Journal of Sound and Vibration* **102**, 329–346. Natural frequencies and mode shapes of an automotive tire with interpretation classification using 3-d computer graphics.
10. Y. Nakajima and J. Padovan 1986 *Tire Science and Technology* **14**, 125–136. Numerical simulation of tire sliding events involving impacts with holes and bumps.
11. L. E. Kung 1990 *SAE Transactions paper no*. 900759 **99**, 1074–1078. Radial vibrations of pneumatic radial tires.
12. R. Takagi and S. Takanari 1991 *SAE Transactions paper no*. 911873 **100**, 987–996.
13. D. S. Stutts, C. M. Krousgrill and W. Soedel 1995 *Journal of Sound and Vibration* **179**, 499–512. Parametric excitation of tire–wheel assemblies by a stiffness non-uniformity.
14. O. A. Olatunbosun and J. W. Dunn 1991 *International Journal of Vehicle Design* **12**, 513–524. Generalized representation of the low frequency radial dynamic parameters of rolling tyres.
15. S. C. Huang and B. S. Hsu 1992 *Journal of Sound and Vibration* **156**, 505–519. An approach to the dynamic analysis of rotating tire–wheel–suspensions units.
16. J. Padovan and O. Paramadilok 1985 *Computers and Structures* **20**, 545–553. Transient and steady state viscoelastic rolling contact.
17. J. T. Oden and T. L. Lin 1986 *Computer Methods in Applied Mechanics and Engineering* **57**, 297–367. On the general rolling contact problem for finite deformations of a viscoelastic cylinder.
18. D. O. Brush and B. O. Almroth 1975 *Buckling of Bars, Plates, and Shells*. New York: McGraw-Hill.
19. L. Meirovitch 1967 *Analytical Methods of Vibration*. London: Macmillan.
20. M. Endo, K. Hatamura, M. Sakata and O. Taniguchi 1984 *Journal of Sound and Vibration* **92**, 261–272. Flexural vibration of a thin rotating ring.
21. D. C. Sorensen 1992 *SIAM Journal on Matrix Analysis and Applications* **13**, 357–385. Implicit application of polynomial filters in a k-step Arnoldi method.

APPENDIX: MATRIX ELEMENTS

The non-zero elements of $\bar{M}$, $\bar{C}$ and $\bar{K}$ can be determined from inspection of equations (68–70) and are given by

$$\bar{M}(1,1) = \rho h/2, \qquad \bar{M}(2n,2n) = \rho h(n^2+1), \qquad \bar{M}(2n+1,2n+1) = \rho h(n^2+1), \tag{A1–A3}$$

$$\bar{M}(2M+2,2M+2) = 2\rho h\gamma, \qquad \bar{M}(2M+3,2M+3) = 2\rho h\gamma, \qquad \bar{M}(2,2M+3) = 2\rho h, \tag{A4–A6}$$

$$\bar{M}(2M+3,2) = 2\rho h, \qquad \bar{M}(3,\ 2M+2) = -2\rho h, \qquad \bar{M}(2M+2,3) = -2\rho h, \tag{A7–A9}$$

$$\bar{C}(1,1) = c_0/2, \qquad \bar{C}(2n,2n) = c_n, \qquad \bar{C}(2n,2n+1) = 2\rho h\Omega n(n^2-1), \tag{A10–A12}$$

$$\bar{C}(2n+1,2n) = -2\rho h\Omega n(n^2-1), \qquad \bar{C}(2n+1,2n+1) = c_n, \tag{A13, A14}$$

$$\bar{C}(2M+2,2M+2) = c_x/(\pi ab), \qquad \bar{C}(2M+3,2M+3) = c_y/(\pi ab), \tag{A15, A16}$$

$$\bar{K}(1,1) = k_0/2, \qquad \bar{K}(2n,2n) = k_n, \qquad \bar{K}(2n,2n+1) = \Omega n c_n, \tag{A17–A19}$$

$$\bar{K}(2n+1,2n) = -\Omega n c_n, \qquad \bar{K}(2n+1,2n+1) = k_n, \tag{A20, A21}$$

$$\bar{K}(2M+2,2M+2) = k_x/(\pi ab), \qquad \bar{K}(2M+3,2M+3) = k_y/(\pi ab), \tag{A22, A23}$$